

Complementary version of INPOP planetary ephemerides, INPOP10b

A. Fienga^{1,2}, J. Laskar¹, A. Verma², P. Kuchynka^{1,3}, H. Manche¹, and M. Gastineau¹

¹ Astronomie et Systèmes Dynamiques, IMCCE-CNRS UMR8028, 77 Av. Denfert-Rochereau, 75014 Paris, France

² Observatoire de Besançon, CNRS UMR6213, 41bis Av. de l'Observatoire, 25000 Besançon, France

³ Jet Propulsion Laboratory, Pasadena, USA

January 12, 2012

Abstract. In this short report, we give results obtained with the new INPOP10b ephemerides, gathering improvement to INPOP10a (3) planetary ephemerides in the asteroid mass determinations and in the extrapolation capabilities. Description of the method newly implemented in INPOP10a for asteroid mass determination is given as well as new masses of minor planets. Improvements in the extrapolation capabilities are also demonstrated.

Key words. celestial mechanics - ephemerides

1. General context

The estimations of the asteroid perturbations on planet orbits are a critical point for the extrapolation capabilities of the planetary ephemerides (19).

The usual approach to this problem has been suggested by (20) and consists of accounting in the dynamical model for a selection of approximately 300 individual asteroids. The masses of the most perturbing asteroids are fitted to observations. For the other objects, masses are deduced from radiometric diameters and the assumption of constant densities within three taxonomic classes. This classic approach has been used in INPOP08 (4) and achieves in terms of the Earth-Mars distance prediction an accuracy of 20 m over 2 years. It is based on an unrealistic hypothesis of constant densities within taxonomic classes. It also relies on an empirical choice of the selection of asteroids to account for and on the choice of the subset of asteroid masses to adjust individually. With INPOP10a, we used an alternative approach(11): approximately 240 asteroids in a list of 287 probable asteroids and a ring should represent the perturbations induced by the main belt on planetary orbits down to an order of a meter. The Bounded Variable Least Squares (BVLS) algorithm developed by (12) is then used in order to fit the masses of all the 287 asteroids listed in (11) with constraints requiring the adjusted masses to be positive or zero. Setting an asteroid mass to zero is equivalent to removing it from the dynamical model. Thus the BVLS algorithm performs simultaneously parameter selection and estimation. From this

method and the original list of 287 asteroids, about 161 asteroid masses were estimated in INPOP10a. We present in the following, a further improvement of the INPOP10a implementation by adding the a priori sigma assumption (17, 18) in the procedure. In section 2, we give the limitation of INPOP10a where in section 3.1, we describe the new approach implemented in INPOP10a and the procedure used for the construction of INPOP10b. New values of asteroid masses obtained during the fit are given in section 3.2. In section 3.3, we demonstrate how INPOP10b is indeed an improvement of INPOP10a for postfit and extrapolated residuals, INPOP10a and INPOP10b being fitted on the same data sample.

2. INPOP10a

INPOP10a is the latest INPOP planetary ephemerides (5,3). It was fitted with the most extended data sample available at the time of its construction in 2010, including Mercury positions deduced from the Messenger spacecraft flybys of Mercury, Saturn positions deduced from the radio and VLBI tracking of the Cassini spacecraft (7, 8), MEX and VEX positions of Mars and Venus (15,16) as well as Jupiter positions deduced from several spacecraft flybys (6).

In using INPOP10a, gravity tests were done (3) as well as asteroid mass determinations. On figure 2 are plotted the distributions of densities deduced from INPOP10a (3), INPOP10b, INPOP08 (4) and from close-encounters and binary systems. Two representations are given: one histogram of density distribution (left-hand side) and one distribution of the density versus the diameters of the ob-

Send offprint requests to: A. Fienga, agnes.fienga@obs-besancon.fr

jects (right-hand side). Are plotted on these figures, only the densities deduced from perturbations bigger than 1 meter on the Mars-Earth distances over the 1970 to 2010 period with error bars representing the 1-sigma uncertainties on the mass determination. The diameters are considered here as perfect. With this optimistic hypothesis, one can first note the smaller uncertainties on the close-encounter estimations compared to those obtained with INPOP. The distributions of the densities are quite different: one should notice an excess of under-estimated masses in INPOP08. In the other hand, the dispersion and the uncertainties of the INPOP10a distribution do not allow to give conclusive remarks even if one can note a diminution of the number of low density objects compared to INPOP08.

Another aspect to consider is the extrapolation capabilities of the ephemerides. As one can notice in figure 3, the extrapolation capabilities of INPOP10a after 2009.8 are quite degraded compared to INPOP08, DE421 (7) or DE423 (10). This can be explained by an over-weighted or over-constrained adjustments of some asteroid masses in INPOP10a.

A new implementation was then necessary

3. INPOP10b

3.1. Modification in the asteroid mass estimations

In order to improve the INPOP extrapolation, we have studied the impact of adding an *a priori* sigma (APS) control (17) to the BVLS algorithm. Such procedure adds stability in the BVLS estimations of the solve-for parameters, and especially in the asteroid mass determination. Such control has been already used for INPOP08 but not associated with the BVLS algorithm. (11) has demonstrated on simulated adjustments that the combination of the two procedures give the best rate of asteroid mass determination. As described in (17) and (18), the APS give supplementary informations related to our best knowledge of the *a priori* value of the solve-for parameters before the fit. Usually they correspond to the *a priori* uncertainties on the solve-for parameters before fitting. With this method, we put more weight on masses which were obtained with a good accuracy by other methods, mainly by close-encounters between 2 asteroids or with one spacecraft and one asteroid or in the case of binary systems. The APS chosen for our study are based on the uncertainties estimated by (Kuchynka et al. 2010): masses obtained with close-encounters have a low uncertainty of about 50% when masses deduced from radiometric measurements of diameters and fixed density have 150% uncertainties. APS are only applied to the determination of asteroid masses. A new adjustment of the initial conditions of the main planet orbits, the mass of the sun, 287 asteroid masses and the mass of an asteroid ring (described in 3) has then been made on the same data sample as INPOP10a. The observational sample stops at 2009.8. The data of Mars orbiter MEX (15,16) obtained after 2009.8 are then not

Table 1. 1- σ dispersion of extrapolated MEX one-way residuals in meters estimated with DE421, DE423, INPOP08, INPOP10a and INPOP10b.

	Extrapolation interval	Time Span in months	MEX residuals 1 σ meters
INPOP10b	2009.8:2011.5	19	5.9
	2009.8:2010.8	12	2.6
INPOP10a	2009.8:2011.5	19	32.4
	2009.8:2010.8	12	14.6
INPOP08	2008.25:2011.5	39	22.7
	2008.25:2009.25	12	11.1
DE423	2009.2: 2011.5	27	8.7
	2009.2:2010.2	12	2.7
DE421	2008:2011.5	42	13.4
	2008:2009	12	4.6

used in the adjustment in order to test the extrapolation of the ephemerides.

3.2. Postfit and extrapolated INPOP10b residuals

The residuals obtained by comparisons between the post 2009.8 range bias and INPOP10a, DE421, DE423 and INPOP10b are given in figure 3. On this figure, the improvement of INPOP10b extrapolation is striking compared to INPOP10a and INPOP08 with no loss of accuracy for the postfit residuals. On table 1 are given the 1- σ deviations of the MEX one-way residuals computed by comparisons between MEX range bias not used in the adjustment of the planetary ephemerides and positions deduced from these ephemerides. In order to give a better view of the extrapolation capabilities of each modele, we also give the residuals obtained after one year of extrapolation. It then appears that INPOP10b has the same quality of extrapolation over one year than DE423, improving the extrapolation capabilities of INPOP10a by a factor 7 over one year and 5 over 19 months. We note the good extrapolated residuals obtained with DE421: as one can see on table 1 and figure 3, these residuals degrade very slowly with time.

3.3. Asteroid mass estimations

A total of 287 asteroid masses selected by (Kuchynka et al. 2010) have been tested: 96 have been rejected from the dynamical modelling (masses put to zero), 71 have reach the maximum bounced value of the BVLS fitting and have then their masses fixed. We then estimated 120 masses. Among these objects, 29 have their masses already estimated with different methods and presented on Table

2 and 75 determinations have uncertainties better than 50%.

Table 1 gives the values of the asteroid masses estimated with INPOP10b and compared with other values obtained with planetary ephemerides or close-encounters. As expected, asteroids with small impacts on the Mars-Earth distances have their masses poorly estimated (130, 253). In the other hand, INPOP10b provides significant estimations (uncertainty better than 50%) for about 75 objects for which the diameter-versus-density distribution is plotted on 2. This sample is twice bigger than the present sample of masses obtained with close-encounters. About 66% of the asteroids which have their masses estimated with INPOP10b have their diameters smaller than 200 kilometers while for masses obtained by close-encounters they represent only 35% of the sample. INPOP10b estimations appear then as a complement to the close-encounters sample for small objects. Besides, the histogram of density for INPOP10b shows an homogeneous distribution of the density when close-encounters distribution of density seems to be biased by a lack of small objects.

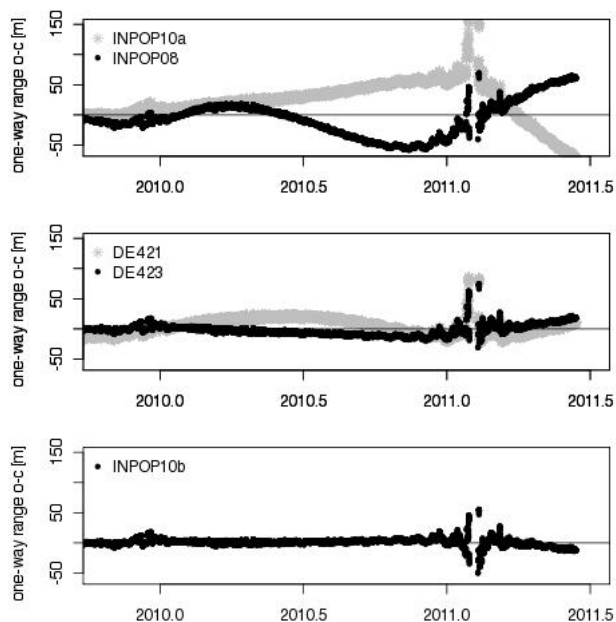


Fig. 3. Extrapolated residuals of MEX range tracking bias obtained with planetary ephemerides.

References

- J. Baer and S. R. Chesley. Astrometric masses of 21 asteroids, and an integrated asteroid ephemeris. *Celestial Mechanics and Dynamical Astronomy*, 100:27–42, January 2008.
- J. Baer, S. R. Chesley, and R. Matson. Astrometric Masses of 28 Asteroids, and Observations on Asteroid Porosity. *AJ*, page in press, 2011.
- A. Fienga, J. Laskar, H. Manche, P. Kuchynka, G. Desvignes, M. Gastineau, and G. Cognard, I. The planetary ephemerides inpop10a and its applications in fundamental physics. *Celestial Mechanics and Dynamical Astronomy*, 2011.
- A. Fienga, J. Laskar, T. Morley, H. Manche, P. Kuchynka, C. Le Poncin-Lafitte, F. Budnik, M. Gastineau, and L. Somenzi. INPOP08, a 4-D planetary ephemeris: from asteroid and time-scale computations to ESA Mars Express and Venus Express contributions. *A&A*, 507:1675–1686, December 2009.
- A. Fienga, H. Manche, P. Kuchynka, J. Laskar, and M. Gastineau. Planetary and Lunar ephemerides, INPOP10A. In *Journées Systèmes de Référence Spatio-temporels 2010*, Journées Systemes de references, November 2010.
- W. M. Folkner, 2010. Private communication.
- W. M. Folkner, J. G. Williams, and D. H. Boggs. Jpl planetary and lunar ephemerides de421. JPL Interoffice Memorandum IOM 343R-08-003, 2008.
- D. L. Jones, E. Fomalont, V. Dhawan, J. Romney, W. M. Folkner, G. Lanyi, J. Border, and R. A. Jacobson. Very Long Baseline Array Astrometric Observations of the Cassini Spacecraft at Saturn. *AJ*, 141:29–+, February 2011.
- O. M. Kochetova. Determination of Large Asteroid Masses by the Dynamical Method. *Solar System Research*, 38:66–75, January 2004.
- A. S. Konopliv, S. W. Asmar, W. M. Folkner, Ö. Karatekin, D. C. Nunes, S. E. Smrekar, C. F. Yoder, and M. T. Zuber. Mars high resolution gravity fields from MRO, Mars seasonal gravity, and other dynamical parameters. *Icarus*, 211:401–428, January 2011.
- P. Kuchynka, J. Laskar, A. Fienga, and H. Manche. A ring as a model of the main belt in planetary ephemerides. *A&A*, 514:A96+, May 2010.
- Charles L. Lawson and Richard J. Hanson. *Solving Least Squares Problems*. SIAM, Philadelphia, PA, 1995.
- F. Marchis, P. Descamps, M. Baek, A. W. Harris, M. Kaasalainen, J. Berthier, D. Hestroffer, and F. Vachier. Main belt binary asteroidal systems with circular mutual orbits. *Icarus*, 196:97–118, July 2008.
- F. Marchis, P. Descamps, J. Berthier, D. Hestroffer, F. Vachier, M. Baek, A. W. Harris, and D. Nesvorný. Main belt binary asteroidal systems with eccentric mutual orbits. *Icarus*, 195:295–316, May 2008.
- T. Morley. Mex and vex data release, 2009. Private communication.
- T. Morley. Mex and vex data release, 2010. Private communication.
- T. Moyer. Dpodp manual. IOM 3215-37, JPL, 1971.
- L. Somenzi, A. Fienga, J. Laskar, and P. Kuchynka. Determination of asteroid masses from their close encounters with mars. *Planetary and Space Science*, 58:858, 2010.
- E. M. Standish and A. Fienga. Accuracy limit of modern ephemerides imposed by the uncertainties in asteroid masses. *A&A*, 384:322–328, March 2002.
- J. G. Williams. Determining asteroid masses from perturbations on Mars. *Icarus*, 57:1–13, January 1984.
- D. K. Yeomans, J.-P. Barriot, D. W. Dunham, R. W. Farquhar, J. D. Giorgini, C. E. Helfrich, A. S. Konopliv, J. V. McAdams, J. K. Miller, W. M. Owen, Jr., D. J. Scheeres, S. P. Synnott, and B. G. Williams. Estimating the Mass of Asteroid 253 Mathilde from Tracking Data During the NEAR Flyby. *Science*, 278:2106–+, December 1997.

Table 2. 29 Asteroid masses found in the recent literature and compared to the values estimated in INPOP10a and INPOP10b. The last column gives the impact of each asteroid on the Earth-Mars distances over the 1970 to 2010 period. The uncertainties are given at 1 published sigma. The star-marked values are fixed masses for INPOP10a

IAU designation number	INPOP10a $10^{12} \times M_{\odot}$	Close-encounters $10^{12} \times M_{\odot}$	Refs	INPOP10b $10^{12} \times M_{\odot}$	Konopliv et al. 11 $10^{12} \times M_{\odot}$	Impact m
1	475.8 ± 2.8	475.700 ± 0.72	2	467.3 ± 1.7	467.900 ± 3.250	794
2	111.4 ± 2.8	101.000 ± 6.5	2	103.8 ± 1.5	103.440 ± 2.550	146
4	133.1 ± 1.7	130.00 ± 0.53	2	130.1 ± 0.6	130.970 ± 2.060	1199
7	7.7 ± 1.1	8.12 ± 0.46	2	5.67 ± 0.4	5.530 ± 1.320	28
324	4.67 ± 0.38			5.7 ± 0.43	5.340 ± 0.990	94
3	11.6 ± 1.3	14.400 ± 2.3	2	11.8 ± 0.6	12.100 ± 0.910	56
6	7.1 ± 1.2	6.40 ± 0.67	2	7.08 ± 0.7	6.730 ± 1.640	21
8	4.07 ± 0.63	3.33 ± 0.42	2	3.35 ± 0.3	2.010 ± 0.420	13
9	5.700 *	5.700 ± 1.1	2	2.99 ± 0.5	3.280 ± 1.080	30
10	44.500 *	43.58 ± 0.74	2	43.5 ± 2.8	44.970 ± 7.760	77
11	1.9 ± 1.0	3.090 ± 0.989		3.8 ± 0.9		17
15	18.8 ± 1.6	15.597 ± 0.15	2	13.58 ± 0.86	14.180 ± 1.490	22
16	11.2 ± 5.2	11.40 ± 0.42	2	12.61 ± 1.83	12.410 ± 3.440	10
19	6.380 *	4.18 ± 0.36	2	4.2 ± 0.3	3.200 ± 0.530	59
21	1.3 ± 1.2	1.31 ± 0.44	2	0.84 ± 0.62		5
24	2.8 ± 1.9	5.670 ± 2.155	1	5.32 ± 2.3		26
29	5.920 *	7.63 ± 0.31	2	7.4 ± 0.85	7.420 ± 1.490	27
31	3.130 *	2.92 ± 0.99	2	4.4 ± 2.0		23
41	9.2 ± 2.6			5.11 ± 0.6	4.240 ± 1.770	12
52	42.3 ± 8.0	11.39 ± 0.79	2	9.0 ± 2.4	11.170 ± 8.400	10
65	7.2 ± 4.2	5.30 ± 0.96	2	8.8 ± 2.6		5
107	18.2 ± 4.6	5.630 ± 0.169	14	13.6 ± 3.5		5
130	11.1 ± 8.0	3.320 ± 0.199	13	0.11 ± 0.06		<1
253	0.904 ± 0.65	0.052 ± 0.002	21	0.6 ± 0.3		<1
451	21.0 ± 14.8	10.2 ± 3.4	9	15.0 ± 3.7		9
511	19.9 ± 4.1	18.96 ± 0.99	2	9.12 ± 2.4	8.580 ± 5.930	34
532	2.89 ± 0.76	16.8 ± 2.8	9	2.89 ± 0.96	4.970 ± 2.810	5
704	18.600 *	19.65 ± 0.89	2	19.2 ± 1.8	19.970 ± 6.570	16
804	2.5 ± 1.8	1.75 ± 0.40	2	3.09 ± 1.2		

Table 3. 46 other asteroid masses deduced from INPOP10b

IAU designation number	INPOP10b $10^{12} \times M_{\odot}$	density g.cm^{-3}	diameter km	IAU designation number	INPOP10b $10^{12} \times M_{\odot}$	density g.cm^{-3}	diameter km
12	1.790 ± 0.258	4.742 ± 0.683	112.76	762	0.556 ± 0.222	0.820 ± 0.327	137.08
17	2.033 ± 0.708	3.861 ± 1.344	126.00	179	0.125 ± 0.060	1.013 ± 0.488	77.68
34	1.851 ± 0.761	4.805 ± 1.974	113.54	194	8.027 ± 0.531	6.383 ± 0.422	168.42
39	2.847 ± 1.032	3.236 ± 1.172	149.52	211	3.936 ± 1.575	5.094 ± 2.039	143.18
42	0.931 ± 0.298	3.515 ± 1.126	100.20	216	2.862 ± 0.892	4.412 ± 1.376	135.06
43	0.522 ± 0.257	6.941 ± 3.409	65.88	240	0.415 ± 0.178	1.406 ± 0.603	103.90
46	2.892 ± 0.617	5.743 ± 1.226	124.14	259	0.187 ± 0.085	0.125 ± 0.057	178.60
47	2.956 ± 1.049	5.487 ± 1.947	126.96	268	3.154 ± 1.219	4.378 ± 1.692	139.88
48	12.062 ± 3.436	4.199 ± 1.196	221.80	328	1.635 ± 0.327	3.345 ± 0.668	122.92
50	0.982 ± 0.366	3.752 ± 1.400	99.82	344	2.036 ± 0.418	3.341 ± 0.687	132.28
51	2.832 ± 0.654	3.328 ± 0.769	147.86	345	1.348 ± 0.595	6.142 ± 2.711	94.12
54	5.159 ± 0.875	4.303 ± 0.730	165.76	356	3.938 ± 0.754	6.606 ± 1.265	131.32
56	2.318 ± 0.485	6.064 ± 1.268	113.24	375	9.456 ± 3.217	6.824 ± 2.321	173.96
59	2.087 ± 0.882	1.772 ± 0.749	164.80	387	0.954 ± 0.320	3.567 ± 1.199	100.52
70	2.177 ± 0.547	4.534 ± 1.139	122.18	410	3.070 ± 0.463	6.183 ± 0.932	123.56
94	5.929 ± 2.191	2.619 ± 0.968	204.88	419	1.230 ± 0.374	2.176 ± 0.661	129.00
96	6.760 ± 1.853	5.226 ± 1.432	170.02	423	3.803 ± 1.749	1.588 ± 0.730	208.78
98	0.741 ± 0.347	2.468 ± 1.158	104.46	469	2.278 ± 0.883	4.372 ± 1.694	125.56
105	1.451 ± 0.424	3.265 ± 0.954	119.08	488	4.914 ± 1.357	5.518 ± 1.524	150.12
127	1.549 ± 0.680	3.519 ± 1.544	118.70	626	1.628 ± 0.654	6.049 ± 2.430	100.74
128	3.365 ± 1.095	1.919 ± 0.625	188.16	702	11.068 ± 2.488	5.695 ± 1.280	194.72
129	1.387 ± 0.451	0.576 ± 0.187	209.16	747	6.702 ± 0.737	5.028 ± 0.553	171.72
152	2.732 ± 0.623	6.471 ± 1.475	117.06	751	1.645 ± 0.293	4.630 ± 0.825	110.5

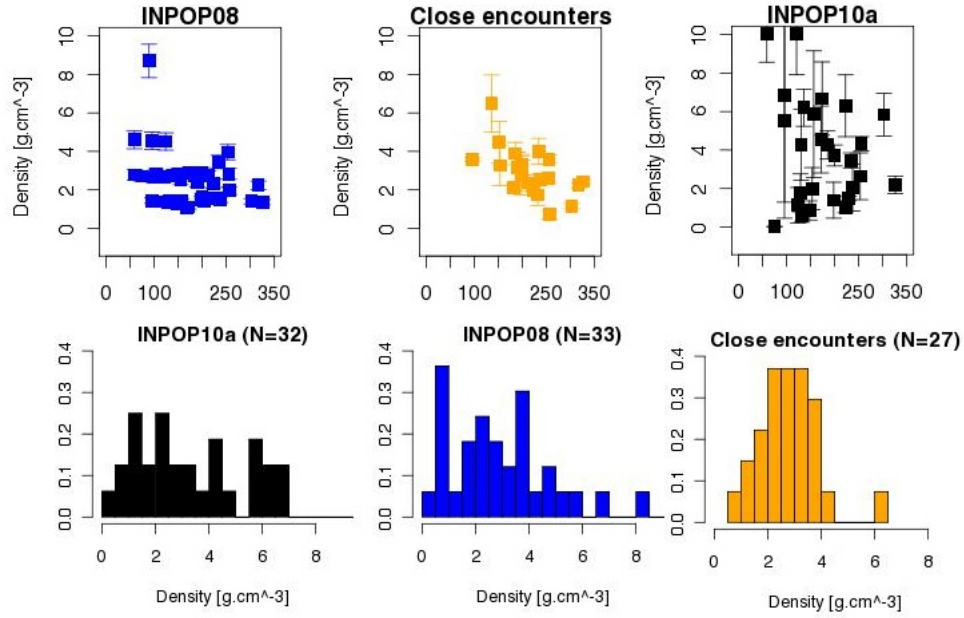


Fig. 1. a) Left-hand side: Histogram of asteroid densities distribution obtained with INPOP10a, INPOP08, INPOP10b and close- encounters ([11]) and IRAS diameters compiled in (11). b) Right-hand side: Distribution of asteroid densities distribution obtained with INPOP10a, INPOP08, INPOP10b and close- encounter masses and IRAS diameters versus diameters in km. The errorbars are with 1-sigma uncertainties of the masses. The diameters are seen as perfect.

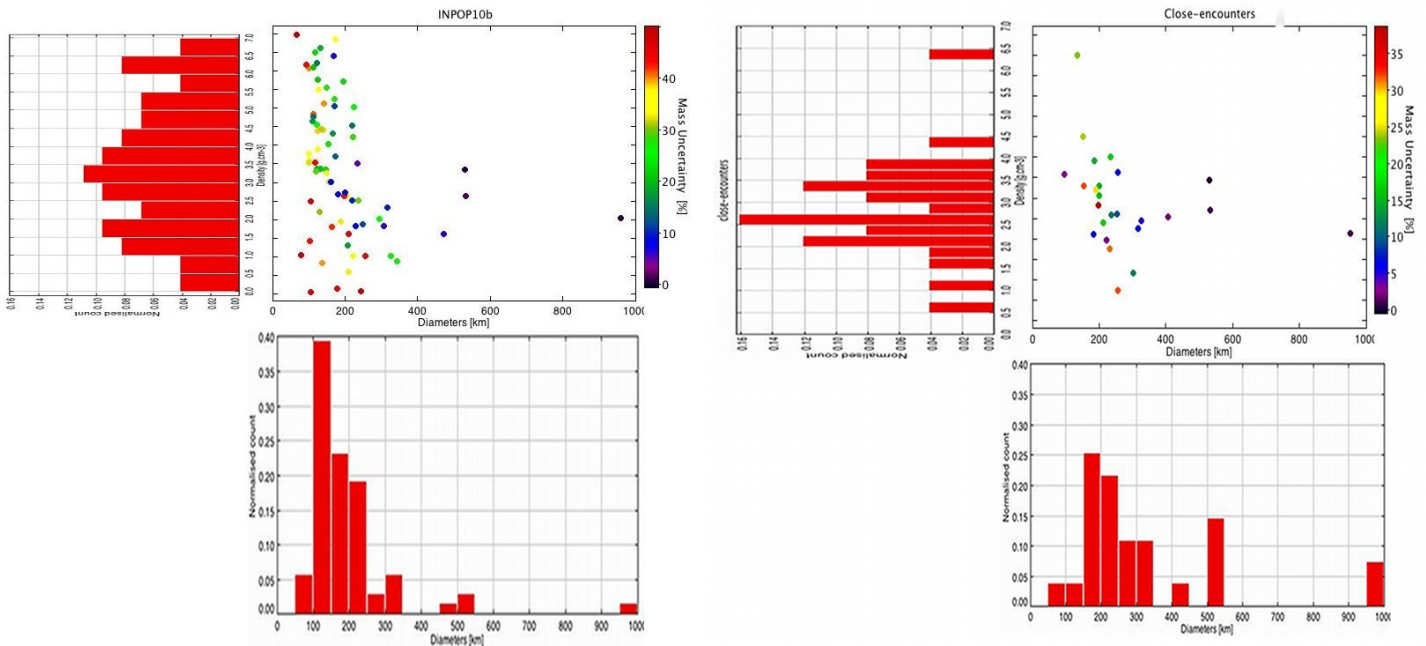


Fig. 2. Distribution in diameters and densities of masses obtained with INPOP10b and close-encounters.